

Article

The correlation between structure and energetic properties of three nitroaromatic compounds: Bis(2,4-dinitrophenyl) ether, Bis(2,4,6-trinitrophenyl) ether and Bis(2,4,6-trinitrophenyl) thioether

Marco Reichel, Dominik Dosch, Thomas Klapoetke, and Konstantin Karaghiosoff

J. Am. Chem. Soc., **Just Accepted Manuscript** • DOI: 10.1021/jacs.9b11086 • Publication Date (Web): 20 Nov 2019

Downloaded from pubs.acs.org on November 23, 2019

Just Accepted

“Just Accepted” manuscripts have been peer-reviewed and accepted for publication. They are posted online prior to technical editing, formatting for publication and author proofing. The American Chemical Society provides “Just Accepted” as a service to the research community to expedite the dissemination of scientific material as soon as possible after acceptance. “Just Accepted” manuscripts appear in full in PDF format accompanied by an HTML abstract. “Just Accepted” manuscripts have been fully peer reviewed, but should not be considered the official version of record. They are citable by the Digital Object Identifier (DOI®). “Just Accepted” is an optional service offered to authors. Therefore, the “Just Accepted” Web site may not include all articles that will be published in the journal. After a manuscript is technically edited and formatted, it will be removed from the “Just Accepted” Web site and published as an ASAP article. Note that technical editing may introduce minor changes to the manuscript text and/or graphics which could affect content, and all legal disclaimers and ethical guidelines that apply to the journal pertain. ACS cannot be held responsible for errors or consequences arising from the use of information contained in these “Just Accepted” manuscripts.

The correlation between structure and energetic properties of three nitroaromatic compounds: Bis(2,4-dinitrophenyl) ether, Bis(2,4,6-trinitrophenyl) ether and Bis(2,4,6-trinitrophenyl) thioether

Marco Reichel,^{†‡} Dominik Dosch,^{†‡} Thomas Klapötke,^{*†} Konstantin Karaghiosoff[†]

[†]Department of Chemistry, Ludwig Maximilian University of Munich, Butenandtstr. 5-13 (D), D-81377 Munich, Germany

Supporting Information Placeholder

ABSTRACT: Decades after the initial discovery of bis(2,4,6-trinitrophenyl) ether (TNB) ether derivatives, the first single-crystal X-ray structures for three members of this compound class could finally be shown and the analytical data could be completed. This group of molecules is an interesting example that illustrates why older predictive models for the sensitivity values of energetic materials like bond dissociation enthalpy and electrostatic potential sometimes give results that deviate significantly from the experimentally determined values. By applying newer models like Hirshfeld surface analysis and fingerprint plot analysis that utilize the crystal-structure of an energetic material, the experimentally found trend of sensitivities could be understood and the older models could be brought into a proper perspective. In the future the prediction of structure-property relationships for energetic molecules starting from a crystal structure can be achieved and should be pursued.

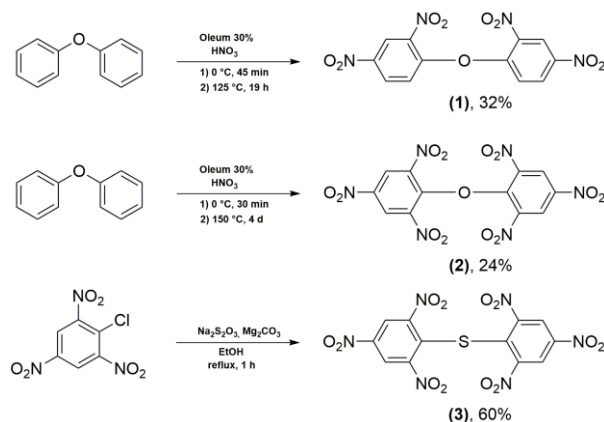
INTRODUCTION

About 150 years ago, Alfred Nobel recognized, that the industrialization of “new” synthetic explosives must be accompanied by their safe handling. The development of dynamite was the first step in this direction.^[1] Just a quarter of a century later, Dynamit Nobel AG focused on TNT, which replaced its predecessors due to its excellent handling safety and brisance.^[2] Although nitroaromatic compounds are no longer the centerpiece of modern explosive investigations,^[3] Alfred Nobel's fundamental aim of increased handling safety that was implemented with this group of materials continues to exist.^[4] The insensitivity to external stimuli is one of the most important requirements for the synthesis of new HEDMs, next to other characteristics such as higher environmental compatibility, high density, high thermal stability and higher detonation velocity/pressure.^[3b, 5] The desired high performance of HEDMs can be achieved by using compounds with a high heat of formation, but these candidates tend to be more sensitive towards external stimuli.^[4a] The contrary behavior of the desired parameters for HEDMs^[4a, 6] leads to the conclusion, that not only the molecular design, but also the crystallographic design has to be considered to find a balance between performance and safety for new energetic materials.^[7] A better visualization and understanding of the sensitizing properties can be achieved by combining older prediction models - such as the calculation of h_{50} values, electrostatic surface potential (ESP) or E_{ES} values^[3b, 4a] - with newer methods like Hirshfeld surface analysis and Fingerprint plot analysis.^[8] After

many years of uncertainty, a deeper insight into the energetic behavior of the title compounds bis(2,4-dinitrophenyl) ether (**1**), bis(2,4,6-trinitrophenyl) ether (**2**) and bis(2,4,6-trinitrophenyl) thioether (**3**), could be gained. This was achieved by combining theoretical methods with structural investigations of the HEDMs to understand the trends that were found for the experimental sensitivity values.

RESULTS AND DISCUSSION

Spectroscopic Characterization. All three compounds were prepared according to modified and optimized methods (Scheme 1).^[9]



Scheme 1. Reaction schemes for compounds (**1**) – (**3**).

Although some of these compounds have existed for almost a century and show some importance today, various fundamental analytical data such as NMR or vibrational spectroscopy are still missing.^[9a, 10] Therefore all three compounds were characterized through multinuclear NMR-, infrared-, Raman spectroscopy, elemental analysis, and single-crystal X-ray diffraction. The ¹H NMR chemical shifts of the proton in ortho position between the NO₂ groups (**1**: 8.9, **2**: 8.6; **3**: 9.1), correspond well with those of 1-substituted trinitro derivatives such as TNT (8.8 ppm) or picric acid (9.0 ppm).^[11] In the ¹³C NMR spectra, the corresponding chemical shifts are observed between 160 ppm and 120 ppm. In the ¹⁴N NMR of **1**, **2** and **3** the differently substituted NO₂ groups are not distinct, due to the signal width of 316 Hz, 280 Hz, and 520 Hz. Characteristic infrared and Raman vibration modes could be assigned according to the literature^[12] and are listed in Table 1.

The substitution of the sulfur in **3** by the more electronegative oxygen in **2** and **1** causes a shift to higher wavenumbers, which is observed for the $\nu(\text{C-N})$ vibration mode. This displacement can be regarded as a measure of the corresponding bond strength. The greater the shift to higher wavenumbers, the stronger the C-N bond. Thus, the bond strength correlates proportionally with the bond dissociation enthalpy (BDE), which – as many researchers have shown – is associated with the sensitivity of energetic materials.^[13] According to this model **3** is expected to have the lowest BDE whereby **2** and **1** should be in a similar range.

Table 1. Characteristic vibration modes of **1**, **2** and **3**.

	1		2		3	
	IR	Raman	IR	Raman	IR	Raman
$\nu(\text{C-H})$	3090	3106	3103	3107	3093	3094
$\nu_{\text{as}}(\text{NO}_2)$	1530	1543	1536	1543	1530	1545
$\nu_{\text{s}}(\text{NO}_2)$	1342	1361	1339	1362	1332	1354
$\nu(\text{C-N})$	913	940	913	941	911	936
$\delta(\text{NO}_2)$	743	796	749	797	748	773

ν_{as} : asymmetric/ symmetric vibration mode; δ : deformation vibration

In this work, the BDEs were calculated from their crystal structure data using the B3LYP/6-311G+(d,p) method, the found values are depicted in Figure 1.



Figure 1. Calculated BDE Values of the weakest Bond in the molecule **1**, **2** and **3**, considering all X-C bonds (X: C, O, N, S)

Since the values of the BDEs for the three compounds all range between RDX (161 kJ mol^{-1}) and TATB (355 kJ mol^{-1}), they can be categorized as sensitive.^[14] The calculated trend of decreasing BDEs from **1** to **3** is consistent with the trend of experimental observation of the shift to higher wavenumbers of the $\nu(\text{C-N})$ vibration mode. As numerous studies have shown, BDEs are considered the most important factor in pyrogenic decomposition for the possible trigger binding that breaks first and can therefore be used to assess the sensitivity of a material.^[7] Besides the calculation of h_{50} values or the determination of *volume-based sensitivities*, the electrostatic potential (ESP) is often used to understand changes of the sensitivities and to visualize the bond strength variation.^[3b]

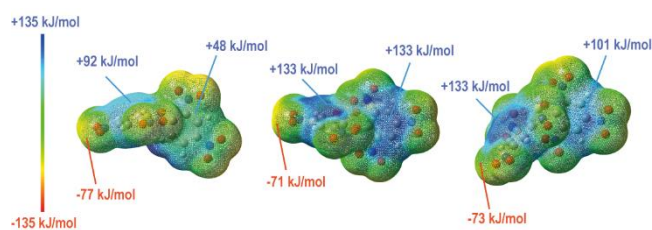


Figure 2. ESP of **1** (left), **2** (center) and **3** (right), calculated on the 0.02 electron bohr⁻³ hypersurface.

The visualization of the ESP for compounds (**1**) – (**3**) is shown in Figure 2. For all compounds, the positive range is larger than the negative range. All positive values are significantly stronger than the negative absolute values. In addition to the strongly positive center of the respective molecules, this is a general indication of their sensitive character.^[3b-d] According to the BDEs and the ESP, the sensitivity of the compounds should increase from **1** to **3**. However, a different trend is present in experimental observations (**1** <

3 < **2**). Thus, these older prediction models are insufficient to explain the actual sensitivities values that were obtained in experiments. In order to explain this, more modern methods that use the crystal structure and packaging effects have to be applied to correctly assess the structure property relationships and therefore the sensitivities of this group of nitroaromatic compounds.

Structure property relationship. In the crystal an external mechanical stimulus like impact or friction can cause a displacement of the layers, which generates internal strains. If this strain energy is below the lowest BDE, the molecular integrity is not destroyed. If the strain energy is higher than the energy required to break the weakest bond the material is destroyed.^[8b] The strain caused by the sliding of the layers depends strongly on the stacking of the layers and other interactions in the crystal, such as hydrogen bridges.^[15]

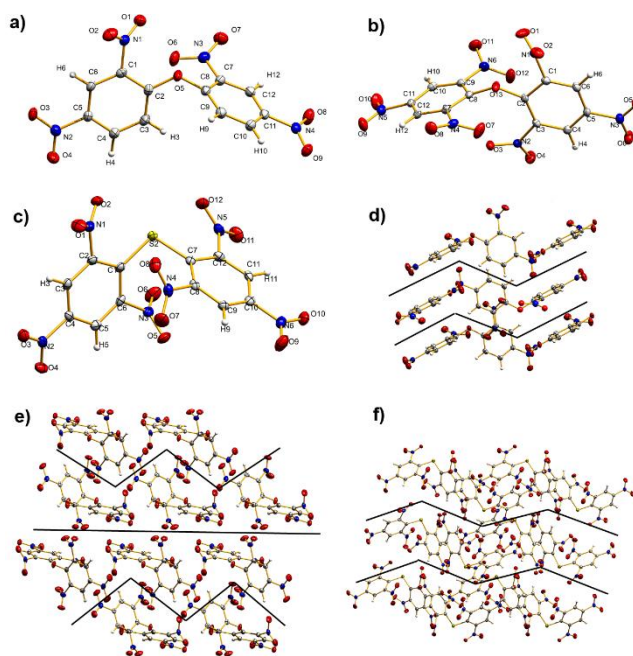


Figure 3. Single-crystal X-ray structure of **1** (a), **2** (b), **3** (c) and the crystal packing of **1** (d), **2** (e), **3** (f).

It can be seen from the monomers a, b and c, that the phenyl residues in the molecules are twisted against each other to different degrees (Figure 3). This results in a different packing behavior in the crystal (d, e, f). The strain energy resulting from a mechanical stimulus should be the greatest for **2**, since the gearing of the individual layers is the highest. The higher interlayer distance which is present in **3** facilitates an easier moving of the layers against each other. This effect can reduce the slip barrier to such an extent that it becomes smaller than the BDE.^[8b] In addition to the lower gearing of **3** versus **2**, this effect is another indication for the higher sensitivity of compound **2** when compared with compound **3**. In addition to crystal packing, intermolecular interactions contribute significantly to the height of the slide barrier and therefore to the sensitivity to external mechanical stimuli. A feature exhibited by insensitive molecules is, that the Hirshfeld surface on a plane has the most red dots representing close contacts.^[15] In the present case all compounds (**1**, **2** and **3**) have red dots which point out of a plane (Figure 4). The close contacts are not arranged in a slideable plane, which results in interlayer repulsion that can be significantly increased by shifting the plane.

The O...O interaction is a very important close contact interaction. In most cases a high frequency of O...O contacts indicates a high sensitivity, because more nitro groups are exposed on the molecular surface and that increases the risk of explosion due to the exceeding

repulsion via an interlayer sliding.^[7, 8b, 14a, 15] Thus, graph d clearly shows that **2** is the most sensitive compound. With 37.9 % of O···O contacts, **2** has the most of those contacts compared to **3** with 33.5 % and **1** with 16.6 %. This distribution can be retrieved from the 2D plot because the marked O···O interactions decrease from a *vi* to *b* in area and color intensity. Furthermore, O···H and N···H contacts, which generate an intermolecular 3D network, can make a compound more sensitive, since an interlayer slide strongly alters these stabilizing interactions. However, the replacement of hard O···O interactions with softer N···H or O···H interactions often leads to a better absorption of mechanical stimuli in a material.^[14a]

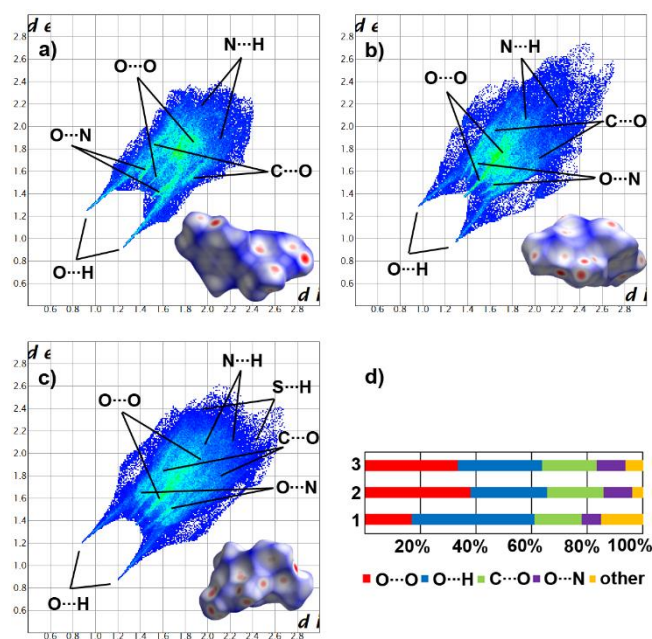


Figure 4. Two dimensional fingerprint plot in crystal stacking as well as the corresponding Hirshfeld surface (bottom right in 2D plot) of **1** (a), **2** (b) and **3** (c) (color coding: white, distance *d* equals VDW distance; blue, *d* exceeds VDW distance, red, *d*, smaller than VDW distance). Population of close contacts of **1**, **2**, and **3** in crystal stacking (d).

Strong O···H and N···H interactions are often found in less sensitive compounds, because the interlayers are more rigid and can absorb energy better without a shifting of the planes, which would induce a repulsion between the layers.^[8b] The 2D fingerprint plot exhibits two distinctive spikes for strong O···H bonding.^[15] With respect to *di* + *de* (*di*: distance from the Hirshfeld surface to the nearest atom interior; *de*: distance from the Hirshfeld surface to the nearest atom exterior) we can ascertain that for **1** with a total of 44.3 % the most and strongest hydrogen bonds are present. For **2** the 27.7 % of H-bridges are the fewest and weakest. With a total of 30.1 %, molecule **3** forms more H-bridges than compound **2** but less than molecule **1** while showing similar strong H-bridges than compound **1**. The interlayer contacts of C···O show weak interactions (distances above 3.5 Å) and therefore can be neglected. This also applies for the N···H and N···O contacts.^[15] According to this newer model the frequencies of O···O contacts and the strength and frequency of H-bridges are the most relevant indicator for the impact sensitivity of an explosive material and therefore the order of decreasing sensitivity for the discussed compounds should be **2** > **3** > **1**.

Heat of formation and detonation parameters. Density plays an important role for the performance of energetic materials and is a direct result of the packing in the crystal. With respect to **1**, **2** and **3**, crystal densities are observed to be 1.73, 1.84 and 1.85 g cm⁻³ at 143 K and the extrapolated values at room temperature are 1.69, 1.80 and 1.81 g cm⁻³. These values deviate significantly from the

older literature values 1.70 (**2**) and 1.61 g cm⁻³ (**3**).^[2] To gain accurate values for the heat of formation (HOF) it is important to use high precision theoretical methods, as experimental values are often inaccurate.^[7] Therefore, the heat of formation was computed by ab initio calculations using the optimized geometry of molecules starting from the X-ray diffraction experiment.

Table 2. Physical and Calculated detonation parameters of compound **1**, **2** and **3** using EXPLO5 computer code.

	1	2	3
formula	C ₁₂ H ₆ N ₄ O ₉	C ₁₂ H ₄ N ₆ O ₁₃	C ₁₂ H ₄ N ₆ O ₁₂ S
<i>M_r</i> [g mol ⁻¹]	350.20	440.19	456.25
<i>I</i> S ^[a] [J]	>40	9	12.5
<i>F</i> S ^[b] [N]	>360	>360	>360
ESD [mJ]	50	50	50
N ^[c] [%]	16.00	19.09	18.42
N + O ^[d] [%]	57.12	66.34	60.50
Ω _{CO₂} ^[e] [%]	-82.24	-47.25	-56.11
<i>T</i> _{mel^[f]} [°C]	246.32	---	253
<i>T</i> _{dec^[g]} [°C]	336.73	256	310
ρ _{143K} ^[h] [g cm ⁻³] (X-ray)	1.73	1.84	1.85
ρ _{298K} ^[i] [g cm ⁻³]	1.68	1.80	1.81
Δ <i>H</i> _f ^[j] [kJ mol ⁻¹]	-168.1	-132.9	-20.3
EXPLO5 V 6.03			
Δ <i>U</i> _f ^[k] [kJ kg ⁻¹]	-3934	-4850	-4689
<i>T</i> _{C-J} ^[l] [K]	2958	3695	2740
<i>P</i> _{C-J} ^[m] [GPa]	16.7	24.9	15.9
<i>V</i> _{det} ^[n] [ms ⁻¹]	6582	7634	6912
<i>V</i> _o ^[o] [dm ³ kg ⁻¹]	582.5	620.4	427.5

[a] Impact sensitivity^[14d] [b] friction sensitivity^[14e] [c] nitrogen content [d] combined nitrogen and oxygen content [e] absolute oxygen balance assuming the formation of CO or CO₂ [f] melting point from DTA [g] decomposition from DTA [h] density determined by X-ray experiment at 143 K [i] ambient temperature density, extrapolated from X-ray value [j] Heat of formation calculated at the CBS-4M level of theory for FMN, experimental determined for MN [k] detonation energy [l] detonation temperature [m] detonation pressure [n] detonation velocity [o] volume of detonation gases at standard temperature and pressure conditions

According to Trouton's Rule, the heat of formation (HOF) was calculated by subtracting the enthalpy of sublimation from the HOF of the corresponding gas-phase species.^[16] The values for the HOF of the gas phase species was obtained by subtraction of the atomization energies from the total enthalpy of the molecule.^[17] Calculations were performed using the CBS-4M level of theory in combination with the crystal structures. By using the specific densities and the EXPLO5 (V6.01) program, the detonation properties of **1**, **2** and **3** could be estimated. They were calculated at the Chapman–Jouguet point (C-J point) with the help of the stationary detonation model using a modified Becker–Kistiakowski–Wilson state equation for gaseous detonation products and the Murnaghan equation of state for condensed products (compressible solids and liquids). By using the first derivative of the Hugoniot curve of the system the C-J point could be found.^[18] Given a high density and heat of formation, it is not surprising that compound **2** exhibits a better performance than **1** and **3**. Although **1** has a higher heat of formation, the influence of the increased density of **2** predominates so strongly that **2** has the best performance. As can be seen in Table 2, the oxygen balance for **1** is lowest due to the lower number of NO₂ groups. The substitution of the ether bridge in **2** by a sulfur atom deteriorates the oxygen balance from **2** to **3** as expected. With respect to the detonation velocity, the values of **2** and **3** exceed TNT (6881 m s⁻¹) were **1** falls below it.

CONCLUSIONS

Bis(2,4-dinitrophenyl) ether, bis(2,4,6-trinitrophenyl) ether, and bis(2,4,6-trinitrophenyl) thioether have been synthesized and characterized. The structures of these three compounds were determined by single-crystal X-ray diffraction. The results of the older

prediction models (BDE, ESP) for the sensitivities were compared with results for newer prediction models based on the crystal structure (Hirshfeld Surface and Fingerprint Plot analysis). The inaccurate trend for the sensitivities that was observed for the older models ($3 > 2 > 1$) could be corrected. The trend for the sensitivities shown by the experimental values (decreasing $2 > 3 > 1$), could be verified by the newer predictive methods which are based on the crystal structure. The application of this newer methods could lead to a better understanding and assessment of sensitivity values without the necessity to synthesize large amounts of new energetic materials, which leads to an increase in safety. The performance of the compounds was calculated and it was found that it decreases from **2** to **3** to **1** with all three compounds showing similar values as TNT.

EXPERIMENTAL SECTION

General Information. Diphenylether, nitric acid, oleum, picryl chloride and sodium thiosulfate were commercially available. For NMR spectroscopy the solvent DMSO- d_6 was dried using 3 Å mole sieve. Spectra were recorded on a Bruker Avance III spectrometer operating at 400.1 MHz (^1H), 100.6 MHz (^{13}C) and 28.9 MHz (^{14}N). Chemical shifts are referred to TMS (^1H , ^{13}C) and MeNO $_2$ (^{14}N). Raman spectra were recorded with a Bruker MultiRam FT Raman spectrometer using a neodymium-doped yttrium aluminum garnet (Nd:YAG) laser ($\lambda = 1064$ nm) with 1074 mW. The samples for Infrared spectroscopy were placed under ambient conditions onto an ATR unit using a Perkin Elmer Spectrum BX II FT-IR System spectrometer. Melting and / or decomposition points were detected with a OZM DTA 552-Ex instrument. The scanning temperature range was set from 293 K to 673 K at a scanning rate of 5 K min^{-1} . Elemental analysis was done with a Vario EL instrument and a Metrohm 888 Titrand device.

Caution! All investigated compounds are explosives, which show partly increased sensitivities toward various stimuli (e.g. higher temperatures, impact, friction or electrostatic discharge). Therefore, proper safety precautions (safety glass, Kevlar gloves and earplugs) have to be applied while synthesizing and handling the described compounds.

Bis(2,4-dinitrophenyl) ether. Diphenylether (2.15 g, 12.65 mmol) was added at 0 °C to a mixed acid consisting of 1.15 mL sulfuric acid, 2.74 mL Oleum (65%) and white fuming nitric acid (2.7 mL, 63.26 mmol). The mixture was stirred for 45 min. After being warmed to room temperature, the solution was heated to 125 °C for 19 hours. The obtained reddish suspension was cooled to room temperature and poured into 750 mL of ice water. The solid was filtered of and washed with water (3 × 100 mL). The filter cake was recrystallized from boiling ethyl acetate and the beige-red powder was dried under ambient conditions (1.4 g, yield: 32%).

^1H NMR (DMSO- d_6 , 400 MHz): δ 7.67 (d, 2H, $J = 2.8$ Hz), 8.60 (dd, 2H, $J = 9.1$, 2.8 Hz), 8.98 (s, 2H, $J = 9.1$ Hz) ppm. ^{13}C NMR (DMSO- d_6 , 100 MHz): δ 151.7, 143.8, 140.3, 130.2, 122.4, 122.3 ppm. ^{14}N (DMSO- d_6 , 29 MHz): δ -20 (s, NO $_2$) ppm. FT-IR (ATR): $\tilde{\nu}$ 3365 (w), 3090 (w), 3076 (w), 2879 (w), 1592 (m), 1530 (s), 1483 (m), 1472 (m), 1422 (w), 1342 (s), 1265 (s), 1155 (w), 1136 (w), 1122 (w), 1067 (s), 972 (w), 928 (m), 913 (s), 867 (s), 834 (s), 787 (w), 762 (w), 743 (s), 721 (s), 687 (w), 661 (m), 639 (m), 603 (w), 521 (w), 499 (w), 458 (w), 435 (w). Raman (1064 nm, 300 mW): $\tilde{\nu}$ 3076 (w), 2263 (w), 2217 (w), 2202 (w), 2157 (w), 2137 (w), 2062 (w), 1951 (w), 1611 (m), 1597 (w), 1547 (w), 1352 (s), 1270 (w), 1213 (w), 1156 (w), 1137 (w), 1066 (w), 838 (m), 641 (w). EA calcd (%) for C $_{12}$ H $_6$ N $_4$ O $_9$: C 41.16, H 1.73, N 16.00; found: C 41.09, H 1.82, N 15.82. DTA: 246 °C (melting), 336 °C (dec) IS: >40.0 J. FS: >360 N. ESD: 50 mJ.

Bis(2,4,6-trinitrophenyl) ether. Diphenylether (1.00 g, 5.88 mmol) was added at 0 °C successively to a mixed acid consisting of 22 mL oleum (30 %) and white fuming nitric acid (4.4 mL, 106 mmol). The mixture was stirred for 30 min. After being warmed to room temperature, the solution was heated to 150 °C for 4 d. The obtained white suspension was cooled to room temperature and poured into 750 mL of ice water. The solid was filtered of and washed with water (3 × 100 mL). The filter cake was recrystallized from boiling chloroform and the colorless powder was dried under ambient conditions (0.53 g, yield: 24%). ^1H NMR (DMSO- d_6 , 400 MHz): δ 8.60 (s, 4H) ppm. ^{13}C NMR (DMSO- d_6 , 100 MHz): δ 160.6, 141.8, 125.2, 124.6 ppm. ^{14}N (DMSO- d_6 , 29 MHz): δ -11 (s, NO $_2$) ppm. FT-IR (ATR): $\tilde{\nu}$ 3103 (m), 1612 (m), 1601 (m), 1536 (s), 1455 (m), 1415 (m), 1339 (s), 1268 (s), 1212 (m), 1191 (m), 1085 (m), 944 (m), 927 (m), 913 (m), 832 (m), 795 (m), 749 (m), 733 (m), 717 (s) 523 (m). Raman (1064 nm, 1074 mW): $\tilde{\nu}$ 3107 (w), 1627 (m), 1559 (m), 1543 (m), 1362 (s), 1275 (w), 1214 (m), 1171 (w), 1083 (w), 941 (w), 829 (m), 797 (w), 329 (w), 270 (w), 202 (w). EA calcd (%) for C $_{12}$ H $_4$ N $_6$ O $_{13}$: C 32.74, H 0.92, N 19.09; found: C 32.71, H 1.01, N 18.88. DTA: 256 °C (dec) IS: 9.0 J. FS: 360 N. ESD: 50 mJ.

Bis(2,4,6-trinitrophenyl) thioether. Sodium thiosulfate (0.498 g, 3.15 mmol) was added successively to a reflux heated suspension of picryl chloride (1.00 g, 4.04 mmol) and magnesium carbonate (0.190 g, 2.26 mmol) in absolute ethanol (25 mL). The mixture was heated for 1 h. The mixture turned into a yellow suspension. After being cooled to room temperature the obtained suspension was filtered of and the filter cake washed with ethanol (3 × 15 mL), 1.0 M HCl (3 × 5 mL) and water (3 × 5 mL). The yellow powder was dried under a nitrogen stream (1.1 g, yield: 60%). ^1H NMR (DMSO- d_6 , 400 MHz): δ 9.17 (s, 4H) ppm. ^{13}C NMR (DMSO- d_6 , 100 MHz): δ 151.6, 147.8, 125.6, 124.4 ppm. ^{14}N (DMSO- d_6 , 29 MHz): δ -19 (s, NO $_2$) ppm. FT-IR (ATR): $\tilde{\nu}$ 3093 (m), 2917 (w), 2850 (w), 1598 (m), 1530 (s), 1392 (w), 1332 (s), 1169 (w), 1112 (w), 1047 (m), 931 (m), 911 (s), 822 (m), 748 (m), 726 (s), 718 (s), 687 (m). Raman (1064 nm, 1074 mW): $\tilde{\nu}$ 3094 (w), 1601 (m), 1545 (m), 1354 (s), 1301 (w), 1180 (m), 1059 (m), 936 (m), 825 (w), 773 (m), 433 (w), 370 (w), 331 (w), 287 (w). EA calcd (%) for C $_{12}$ H $_4$ N $_6$ O $_{12}$ S: C 31.59, H 0.88, N 18.42, S 7.03; found: C 31.48, H 0.94, N 18.34, S 7.17. DTA: 253 °C (mp), 310 °C (dec) IS: 12.5 J. FS: 360 N. ESD: 50 mJ.

X-Ray Measurements. Bis(2,4,6-trinitrophenyl) ether and bis(2,4-dinitrophenyl) ether were solved in ethylacetate and single crystals have been received after slow solvent evaporation. Single crystals of bis(2,4,6-trinitrophenyl) thioether have been received of the decomposition of fluoromethyl-(2,4,6)-trinitrobenzene sulfonate with triphenylphosphine sulfid in DCM after slow solvent evaporation. Data collection was performed with an Oxford Xcalibur3 diffractometer with a CCD area detector, equipped with a multilayer monochromator, a Photon 2 detector and a rotating-anode generator were employed for data collection using Mo-K α radiation ($\lambda = 0.7107$ Å). Data collection and reduction were carried out using the CrysAlispro software.^[19] The structures were solved by direct methods (SIR-2014)^[20] and refined (SHELXLE)^[21] by full-matrix least-squares on F2 (ShelxL)^[(22)|(23)] and finally checked using the platon software^[24] integrated in the WinGX software suite.^[25] The non-hydrogen atoms were refined anisotropically and the hydrogen atoms were located and freely refined. All Diamond 3 plots are shown with thermal ellipsoids at the 50% probability

level and hydrogen atoms are shown as small spheres of arbitrary radius.

ASSOCIATED CONTENT

Supporting Information

The Supporting Information is available free of charge on the ACS Publication website.

¹H, ¹³C, ¹⁴N NMR spectra; Detonation parameter calculations (output files) (PDF)

X-ray data for bis(2,4-dinitrophenyl) ether (CIF)

CCDC: 1959182

X-ray data for bis(2,4,6-trinitrophenyl) ether (CIF)

CCDC: 1959183

X-ray data for bis(2,4,6-trinitrophenyl) thioether (CIF)

CCDC: 1959184

AUTHOR INFORMATION

Corresponding Author

* tmk@cup.uni-muenchen.de

ORCID

Konstantin Karaghiosoff: 0000-0002-8855-730X

Thomas Klapötke: 0000-0003-3276-1157

Marco Reichel: 0000-0003-0137-4816

Dominik Dosch: 0000-0003-4804-6473

Author Contributions

‡ Marco Reichel and Dominik Dosch contributed equally to this work.

Notes

The authors declare no competing financial interests.

ACKNOWLEDGMENT

For financial support of this work by Ludwig–Maximilian University (LMU), the Office of Naval Research (ONR) under grant no. ONR.N00014-16-1-2062 and the Strategic Environmental Research and Development Program (SERDP) under contract no. WP19-1287 are gratefully acknowledged. The authors also thank Ms. Teresa Küblböck for help with the graphics and F–Select GmbH for the generous donation of fluoro-chemicals.

REFERENCES

- [1] Nobel, A. *Dynamit*. United Kingdom, **1867**.
- [2] a) Köhler, J.; Meyer, R.; Homburg, A. *Explosivstoffe*, Wiley-VCH, **2008**, Weinheim; b) Klapötke, T. M. *Energetic Materials Encyclopedia*, De Gruyter, 1st edn., **2018**, Boston/Berlin.
- [3] a) Giles, J. Green explosives: collateral damage. *Nature* **2004**, *427*, 580-581; b) Klapötke, T. M. *Chemistry of High-Energy Materials*, De Gruyter, 5th edn., **2019**, Boston/Berlin c) Reichel, M.; Krumm, B.; Vishnevskiy, Y.; Blomeyer, S.; Schwabedissen, J.; Stammler, H.-G.; Karaghiosoff, K.; Mitzel, N. W. *Angew. Chem. Int. Ed.* **2019**, *in Press* (DOI: 10.1002/anie.201911300); d) Reichel, M.; Krumm, B.; Karaghiosoff, K. Synthesis and investigation of highly energetic and shock-sensitive fluoromethyl perchlorate. *J. Fluorine Chem.* **2019**, *226*, 109351.
- [4] a) Zhi, C.-Y.; Cheng, X.-L.; Zhao, F. The Correlation between Electric Spark Sensitivity of Polynitroaromatic Compounds and Their Molecular Electronic Properties. *Propellants, Explos., Pyrotech.* **2010**, *35*, 555-560; b) Zeman, S.; Krupka, M. New aspects of impact reactivity of polynitro compounds, part III. Impact sensitivity as a function of the intermolecular interactions. *Propellants, Explos., Pyrotech.* **2003**, *28*, 301-307; c) Tan, B.; Li, H.; Huang, H.; Han, Y.; Li, J.; Li, M.; Long, X. Large π - π separation energies of some energetic compounds. *Chem. Phys.* **2019**, *520*, 81-87.
- [5] Gao, H.; Shreeve, J. Azole-Based Energetic Salts. *Chem. Rev. (Washington, DC, U. S.)* **2011**, *111*, 7377-7436.
- [6] Thottempudi, V.; Gao, H.; Shreeve, J. Trinitromethyl-substituted 5-nitro- or 3-azo-1,2,4-triazoles: synthesis, characterization, and energetic properties. *J. Am. Chem. Soc.* **2011**, *133*, 6464-6471.
- [7] Zhang, J.; Zhang, Q.; Vo, T. T.; Parrish, D. A.; Shreeve, J. Energetic Salts with π -Stacking and Hydrogen-Bonding Interactions Lead the Way to Future Energetic Materials. *Journal of the American Chemical Society* **2015**, *137*, 1697-1704.
- [8] a) Spackman, M. A.; Jayatilaka, D. Hirshfeld surface analysis. *CrystEngComm* **2009**, *11*, 19-32; b) Ma, Y.; Zhang, A.; Xue, X.; Jiang, D.; Zhu, Y.; Zhang, C. Crystal Packing of Impact-Sensitive High-Energy Explosives. *Cryst. Growth Des.* **2014**, *14*, 6101-6114.
- [9] a) Rath, C.; Rost, A.; Rittler, K. W. Hexanitrodiphenyl ether. *Chemische Fabrik von Heyden A.-G.* **1936**; b) Sprengstoff-A.-G. Carbonit. **1912**.
- [10] a) Isanbor, C.; Emokpae, T. A. Anilinolysis of nitro-substituted diphenyl ethers in acetonitrile: The effect of some ortho-substituents on the mechanism of SNAr reactions. *Int. J. Chem. Kinet.* **2009**, *42*, 37-49; b) Davydov, D. V.; Mikaya, A. I.; Zaikin, V. G. Mass-spectrometric study of substituted trinitrobenzenes. *Zh. Obshch. Khim.* **1983**, *53*, 455-462; c) Desvergnès, L. Some physical properties of nitro derivatives. *Monit. Sci. Doct. Quesneville* **1926**, *16*, 201-208; d) Zhou, J.; Zhang, C.; Wang, Y.; Zhang, M.; Li, Y.; Huang, F.; Hu, L.; Xi, W.; Wang, Q. 2,2',4,4',6,6'-hexanitrodiphenyl sulfide refining method. *Modern Chemistry Research Institute, Peop. Rep. China* **2015**, p. 6pp.
- [11] a) Hussain, I.; Tariq, M. I.; Siddiqui, H. L. Structure elucidation of chromogen resulting from Jaffe's reaction. *J. Chem. Soc. Pak.* **2009**, *31*, 937-948; b) Soojhawon, I.; Lokhande, P. D.; Kodam, K. M.; Gawai, K. R. Biotransformation of nitroaromatics and their effects on mixed function oxidase system. *Enzyme Microb. Technol.* **2005**, *37*, 527-533.
- [12] Lewis, I. R.; Daniel, N. W.; Griffiths, P. R. Interpretation of Raman spectra of nitro-containing explosive materials. Part I: Group frequency and structural class membership. *Appl. Spectrosc.* **1997**, *51*, 1854-1867.
- [13] a) Li, J. Relationships for the Impact Sensitivities of Energetic C-Nitro Compounds Based on Bond Dissociation Energy. *J. Phys. Chem. B* **2010**, *114*, 2198-2202; b) Li, J. A quantitative relationship for the shock sensitivities of energetic compounds based on X-NO₂ (X = C, N, O) bond dissociation energy. *J. Hazard. Mater.* **2010**, *180*, 768-772.
- [14] a) Tang, Y.; Zhang, J.; Mitchell, L. A.; Parrish, D. A.; Shreeve, J. Taming of 3,4-Di(nitramino)furan. *J. Am. Chem. Soc.* **2015**, *137*, 15984-15987; b) Test methods according to the UN Manual of Tests and Criteria, Recommendations on the Transport of Dangerous Goods, N. Y. United Nations Publication, Geneva, 4th

- revised ed., 2003: Impact: insensitive >40 J, less sensitive ≥ 35 J, sensitive ≥ 4 J, very sensitive ≤ 3 J; friction: insensitive >360 N, less sensitive: 360 N, sensitive <360 N and >80 N, very sensitive ≤ 80 N, extremely sensitive ≤ 10 N; c) www.reichel-partner.com; d) NATO, Standardization Agreement 4489 (STANAG 4489), Explosives, Impact Sensitivity Tests. Brussels, Belgium **1999**; e) NATO, Standardization Agreement 4487 (STANAG 4487), Explosives, Friction Sensitivity Tests. Brussels, Belgium **2002**.
- [15] Zhang, C.; Xue, X.; Cao, Y.; Zhou, Y.; Li, H.; Zhou, J.; Gao, T. Intermolecular friction symbol derived from crystal information. *CrystEngComm* **2013**, *15*, 6837-6844.
- [16] Klapötke, T. M. *Chemie der hochenergetischen Materialien*, De Gruyter, **2009**, Boston/Berlin.
- [17] a) Curtiss, L. A.; Raghavachari, K.; Redfern, P. C.; Pople, J. A. Assessment of Gaussian-2 and density functional theories for the computation of enthalpies of formation. *J. Chem. Phys.* **1997**, *106*, 1063-1079; b) Byrd, E.; Rice, B. M. Improved Prediction of Heats of Formation of Energetic Materials Using Quantum Mechanical Calculations. *J. Phys. Chem. A* **2006**, *110*, 1005-1013.
- [18] a) Suceska, M. *EXPLO5 6.01* **2013**, Brodarski Institute: Zagreb, Croatia; b) Klapoetke, T. M.; Krumm, B.; Steemann, F. X.; Umland, K.-D. Bis(1,3-dinitratoprop-2-yl) nitramine, a new sensitive explosive combining a nitrate ester with a nitramine. *Z. Anorg. Allg. Chem.* **2010**, *636*, 2343-2346.
- [19] CrysAlisPRO (Version 171.33.41), **2009**, Oxford Diffraction Ltd.
- [20] Burla, M. C.; Caliandro, R.; Carrozzini, B.; Cascarano, G. L.; Cuocci, C.; Giacovazzo, C.; Mallamo, M.; Mazzzone, A.; Polidori, G., Crystal structure determination and refinement via SIR2014. *J. Appl. Crystallogr.* **2015**, *48*, 306.
- [21] Hübschle, C.B., Sheldrick, G.M., Dittrich B. ShelXle: a Qt graphical user interface for SHELXL. *J. Appl. Cryst.* **2011**, *44*, 1281.
- [22] Sheldrick, G. M., SHELXL-97, Program for the Refinement of Crystal Structures., **1997** University of Göttingen, Germany.
- [23] Sheldrick, M. A short history of SHELX. *Acta Crystallogr. Sect. A* **2008**, 112.
- [24] Spek, A. L., PLATON, A Multipurpose Crystallographic Tool., **1991**, Utrecht University, The Netherlands.
- [25] Farrugia, L. J., WinGX and ORTEP for Windows: an update. *J. Appl. Cryst.* **2012**, 849.

1
2
3
4
5
6
7
8
9
10
11
12
13
14
15
16
17
18
19
20
21
22
23
24
25
26
27
28
29
30
31
32
33
34
35
36
37
38
39
40
41
42
43
44
45
46
47
48
49
50
51
52
53
54
55
56
57
58
59
60

